Study on the compatibility of unbleached and bleached bamboo-fiber with LLDPE matrix

Sandeep Kumar · Veena Choudhary ·
Rakesh Kumar

Abstract This article presents the comparative study on the compatibility of unbleached and bleached bamboo-fibers (UBF and BBF) with LLDPE matrix. Thermal characterization of composites was conducted by differential scanning calorimetry and thermogravimetric analysis. The results suggested that BBF are more compatible with matrix than the unbleached ones. The X-ray diffraction pattern shows no change in the intensity peak position of matrix in the presence of bamboo fibers. Morphological studies were done by scanning electron microscopy to get an idea of the compatibility of the fibers with the matrix. This study gives us the idea of using the bleached fiber for the preparation of the composites.

Keywords LLDPE · Compatibility · Bamboo-fiber · Bleaching · Thermal characterization

Introduction

Polymer composites based on natural fibers are currently attracting great attention as alternative materials to glass or synthetic fiber reinforced plastics in several applications, mostly for automotive, appliance, and packaging products. The main advantage of employing natural fibers is that these are biodegradable and renewable, and exhibit low cost, low density and high toughness. However, the low compatibility between fibers and polymer matrix generally leads to weak mechanical performances, limiting the use of these materials. In order to improve the interfacial interactions between the components, surface modification of the fibers and/or polymer functionalization, as well as addition of compatibilizers is required [1, 2].

The compatibility of natural fibers composites depends on the interaction between the fibers and matrix which ultimately depends on the chemical structure of fibers. In the case of polymer blends containing crystalline polymer, the melting and crystallization temperature depression was observed by mixing with other polymers [3]. The compatibility affects the percentage crystallinity, mechanical properties, thermal stabilities, and other thermal related properties. A significant literature was found on the thermal study of natural fiber (NF) and flour (like wood, wheat straw, etc.) composites [4–7]. Habibi et al. [8] used the differential scanning calorimetry (DSC) to study the thermal properties of lignocellulosic fibers composites. Thermal decomposition behavior of various natural fibers including bamboo-fibers (BFs) was studied by using thermogravimetric (TG) analysis [9].

Among the well-known natural fibers (jute, coir, straw, banana, etc.), bamboo has low density and high mechanical strength. The specific tensile strength and specific gravity of BFs are considerably less than those of glass fibers. However, cost considerations make bamboo an attractive fiber for reinforcement [10]. Despande et al. [11] explored the compression molding technique (CMT) and roller mill technique (RMT) in combination with the alkaline treatment for extracting the BF. Okubo et al. [12] used mechanically rubbing to reduce diameter 10–30 μm after steam explosion technique for the extraction of BF as reinforcement for polypropylene (PP). These techniques give fiber bundles which create a problem in dispersion

S. Kumar (✉) · V. Choudhary
Centre for Polymer Science and Engineering, Indian Institute
of Technology, Delhi, Hauz Khas, New Delhi 110016, India
e-mail: sanju_chemiit@yahoo.co.in

R. Kumar
CSIR Materials Science and Manufacturing, P.O. Box 1124,
Port Elizabeth 6000, South Africa

with polymer matrix while single fiber is desirable for better dispersion.

Therefore, the objective of this study was to investigate the chemical treatment so that fiber extraction technique could easily separate fiber bundles into single fiber. Furthermore, this article reports on the application of DSC and TG techniques to compare the compatibility of the BF-filled composites without compatibilizer. The morphological characterization was also done to verify the DSC and TG results about the compatibility of fibers with matrix and was correlated with X-ray diffraction and water sorption results.

Experimental

Materials

LLDPE (G-Lene) with 0.9 g/10 min MFI and 0.92 g cm^{-3} density was purchased from GAIL (India) Limited. The fibers of *Ochlandra travancorica* (1 year old), bamboo species grown in India, was used for composite preparation. The method to obtain unbleached bamboo-fiber (UBF), brown in color, is shown in Fig. 1. In the typical process, bamboo was chopped into chips (4 × 1.5 × 0.7 inch^3 size) and was boiled with 4% (mass/volume) sodium hydroxide (1:30::material:liquor ratio) for 2 h, with the repetition of three to five times for fiber extraction, under a pressure of 1 × 10^5 Pa while Deshpande et al. [11] used alkaline treatment by soaking of bamboo strips in 0.1% NaOH for 72 h for the extraction of fibers. The chemical constituent of bamboo can be classified into around: 2.6% extractives, 25.5% lignin, 45.3% alpha-cellulose, and 24.3% polyoses and the alkali treatment removed polysaccharides plus lignin [13]. 38–42% of these substances from bamboo were removed on the mass basis of bamboo chips by delignification process. Pulp obtained was cooled, filtered, washed with water, redistributed in water, and then treated with glacial acetic acid till it reaches 3–4 pH. The pulp was filtered and broken into strands manually. It was thoroughly washed with water. The UBF was dried off in sun and then in an oven for 8 h at 105 °C to expel the moisture before they were used for the fabrication of composites. The problem of this method is that some fiber bundles of diameter 100 ± 10.4 μm were also formed during extraction. Alkaline treatment was used only as a tool for facilitation of UBF extraction. Therefore, the parameters were chosen to optimize separation of BFs by using minimum amount of NaOH.

Sodium chlorite was used to obtain bleached bamboo-fibers (BBF), white in color, as procedure shown in Fig. 2. Delignified bamboo strands were bleached with boiling 4% (mass/volume) sodium chlorite at boil for 1 h duration. The material-to-liquor ratio employed was 1:40. Formic acid was added to maintain an acidic pH in the range 3–4. The fibers were then thoroughly washed with water and dried in the same way as described for UBF. Around 2% mass loss and white color of the fiber was observed during bleaching process. This may be attributed to an oxidizing effect of sodium chlorite on many of the natural waxes and pectins found in cellulose fibers, and on lignin moiety [14]. Sodium chlorite helps to solubilize them and makes the fiber more even and workable. It has the added benefit of destroying natural color matter without attacking the fibers themselves. This makes it useful for making permanent white fibers without compromising tensile
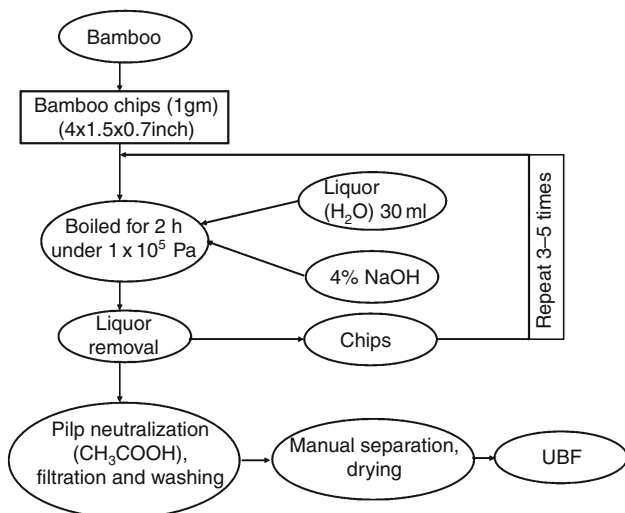

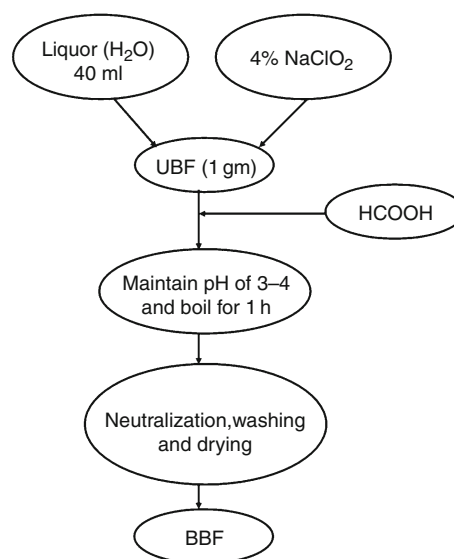Fig. 1 Method for obtaining unbleached bamboo-fibers

Fig. 2 Method for getting bleached bamboo-fibers

Table 1 Physical properties of fibers

Properties of fibers	*Ochlandra travancorica* (1-year-old)	
	Bleached fiber	Unbleached fiber
Length/mm	5 ± 1 (bleaching) 1.5 ± 1 (trace analyzer)	35 ± 5 (delignification) 1 ± 1.5 (scission)
Diameter/μm	10 ± 2.1	17 ± 3.4
Density/gm cm^{-3}	0.94	0.81
Moisture present/%	6–6.7	9–9.8
Moisture regain/%	8–8.6	11–11.8

strength. Food-processing companies use it for washing fruits and vegetables, and meat because it is a fungicide [15–17]. The properties of the natural fibers are dependent mainly on the source, age and separating techniques of the fiber [18]. The BBF lumps were opened manually and the trace analyzer machine was used to separate the discontinuous-short fibers and long fibers in their respective chamber and then collected to use for the reinforcement in polymeric matrix. The physical properties of bamboo-fibers (UBF/BBF) are given in Table 1. The length and diameter of the fibers are measured manually and by using optical microscope, LEICA, at a magnification of 100×, respectively by taking the average reading of 20 samples. Density of the fibers is determined by density bottle method. The presence of moisture in the fibers is measured under normal atmospheric conditions on a mass basis by taking five readings. Moisture regain is measured by Sartorius Moisture Analyzer MA 30 with fibers being conditioned at 65% RH, 24 °C in a desiccators containing saturated sodium nitrite for more than 48 h prior to testing. An average of five readings was taken to compute the mean moisture regain. Moisture present, and moisture regain was lower in BBF because of bleaching as it removes the amorphous natural color matter and gives less opportunity for water molecules to enter into the fibers.

Preparation of composites

The HAAKE Rheomix 600, equipped with a roller mixer-measure head with precisely controlled temperature and rotation speed, was used to disperse the fibers within LLDPE matrix. The torque and melt temperature were monitored on-line and recorded for all composite samples. LLDPE composite sheets using fiber as reinforcement were prepared by compression molding (CARVER) at 190 °C under 5 ton pressure for 15 min by using a 140 × 120 × 3 mm stainless steel mold. After cooling the sheets under pressure were removed and cut for further testing. Pure LLDPE has been designated as LLDPE and composite samples prepared by mixing 10, 20, 30, 40, and 50% (mass/mass) of UBF/BBF have been designated as LU or LB followed by the numerical suffix representing the percent of BF. For example, samples prepared by mixing 10 and 20% of UBF/BBF have been designated as LU-10 and LU-20/LB-10 and LB-20, respectively.

Characterization

Thermal stability of BF, LLDPE, and BF-filled composites was determined by recording TG/derivative of thermogravimetric (DTG) traces in nitrogen atmosphere. Perkin Elmer pyris 6 having TG module was used. Dynamic scans were run from room temperature to 700 °C at a heating rate of 20 °C min^{-1}. The average mass of samples tested was 10 ± 2 mg used in each experiment. To get consistency in the results, each experiment was repeated three times. The residual mass measured during the TG test was converted to the corresponding value of percentage of the residual mass fraction [w_r (%) = 100 w_t/w_0] where w_t is the mass of the sample at each temperature and w_0 is the initial mass of the sample. DTG curves were obtained in order to compare the mass loss rate during the temperature scan [19]. The temperature at which the slope of the mass versus temperature curve starts to decrease was noted as the temperature of the degradation initiation (TDI).

Crystallization and melting behavior was studied by DSC. Perkin Elmer pyris 6 was used for recording DSC scans. The samples having size of 5 ± 2 mg was, used in each experiment, heated to 150 °C at a rate of 20 °C min^{-1} in BF/LLDPE composites, and kept for 3 min to remove the thermal history. Then, the samples were cooled to 40 °C at a cooling rate of 10 °C min^{-1}, and heated again to 150 °C at the rate of 10 °C min^{-1}. The exothermic and endothermic peaks were termed as crystallization temperature (T_c) and melting endotherm (T_m). The crystallization enthalpy (ΔH_c) and the heat of fusion (ΔH_f) were also determined from the area of crystallization and melting peaks, respectively. The maximum temperature limits for the scan were chosen based on the melting range of LLDPE. The crystallinity index (CI$_{DSC}$) of LLDPE was calculated according to the following equation [20]:

$$CI_{DSC}(\%) = \frac{\Delta H_f \times 100}{\Delta H_{100} \times w_{LLDPE}}$$

where ΔH_f is the heat of fusion of the LLDPE and composites, ΔH_{100} the heat of fusion for 100% crystalline LLDPE and w_{LLDPE} is the mass fraction for LLDPE in the composites. The heat of fusion of 100% crystalline LLDPE (140.6 J gm^{-1}) is taken from literature [21, 22] and the CI_{DSC} was calculated. X-ray diffractograms [scan range $(2\theta) = 10°-35°$, θ diffraction angle, scan speed 5° min^{-1}] of the UBF/LLDPE composite samples were obtained with a PANalytical X-ray diffractometer having an X-ray tube producing monochromatic CuKα radiation. The powdered fiber samples (UBF/BBF) and composite sheets were mounted onto sample stage to record the diffraction patterns. Sample stage was mounted on horizontal axis and the diffracted beam optics and the detector was mounted onto 2θ axis. The curves were then analyzed for crystallinity. The % crystallinity was estimated using equation:

$$Crystallinity\ (\%) = \left(\frac{Crystalline\ area}{Total\ area}\right) \times 100.$$

Tensile properties were measured by using Zwick (Z010) machine model. Tensile specimens (dumbbell shaped) of 25 mm gaze length were cut from the molded sheets according to ASTM standard D638-03 type 1 V. The cross-head speed of 100 and 5 mm min^{-1} was used for LLDPE and its composites, respectively.

The composites sample was fractured in liquid nitrogen and fractured surface was analyzed using scanning electron microscopy (SEM) (Cambridge stereoscan 360) after coating with gold to avoid the electrostatic charging and poor image resolution.

Dog-bone shaped specimens of composite with dimensions $60 \times 12 \times 3$ mm^3 were immersed in water at room temperature (30 °C). In general, absorption of water causes swelling of the fibers-this leads to dimensional instability

in the final composite product made of natural fiber as reinforcing phase. Hence, water uptake is very important phenomenon in natural fiber composites. Mass change of the samples was recorded using an electronic balance at regular time intervals. The water uptake in the samples was periodically measured for up to 1,600 h of soaking. The moisture uptake expressed in percent mass gain, $\Delta M\ (t)$, is

$$\Delta M(t) = \left(\frac{M_t - M_0}{M_0}\right) \times 100$$

where M_0 and M_t are the mass of the specimens before and during water uptake, respectively.

Results and discussion

Thermal stability

There were two thermal degradation stages for the composite systems containing natural fibers. One degradation stage was for the LLDPE decomposition, and the other was for the fibers. The first stage of degradation was depending on the BFs encapsulation and interaction with matrix. Figure 3 shows the TG/DTG traces of BF, LLDPE and their composite samples with varying fiber content. We can compare thermal stability by onset temperature but there was no effect with the addition of BF on the onset temperature. So, we can determine the thermal stability by comparing the TDI. Single step mass loss decomposition was observed in case of BF (lower temperature) and LLDPE (higher temperature) whereas all the composites showed two steps decomposition. In BF, one step decomposition, i.e., in the temperature range of 250–400 °C (due to thermal degradation of cellulose and lignin moiety) was observed. This degradation was confirmed by the peak in the DTG traces. The char yield in all composites increased from 1.25 to 3.75% in UBF/LLDPE composites and from

Fig. 3 TG (a, c) and DTG curves (b, d) of UBF/LLDPE (a, b) and BBF/LLDPE composites (c, d)
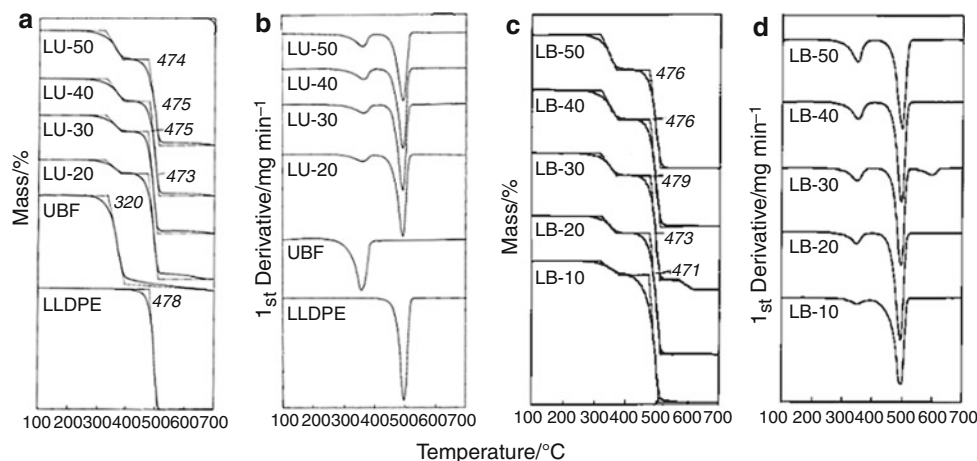
1.25 to 5% in BBF/LLDPE composites as a function of fiber content. The higher char yield in BBF/LLDPE could be due to more physical interaction between BBF and LLDPE owing to larger surface area of BBF and may be because of better encapsulation of fiber by matrix due to removal of higher water absorbing substances. LLDPE alone showed single step decomposition in the temperature range of 400–500 °C with no trace of char. In case of BF reinforced LLDPE composites, first mass loss step was in the temperature range of 270–400 °C (assigned to decomposition of cellulose/lignin) and then second step in the temperature range 410–510 °C that can be assigned for the decomposition of LLDPE.

The TDI of BF increased from 228 (for UBF) to 255 °C for UBF/LLDPE composites and to 280 °C for BBF/LLDPE composites. This could be due to good compatibility of BF in the matrix and encapsulation of fibers by the matrix. The TDI for BBF/LLDPE composites was higher because of good holding capacity or may be better compatibility of LLDPE matrix to BBF. The rate of initial mass loss increased with the addition of BF but still lower in case of unbleached fibers because of the presence of lignin moiety.

Crystallization and melting behavior

Compatibility of bamboo-fiber (UBF/BBF) and crystallinity index

Figure 4 shows the DSC melting curves, obtained during the first (a), and second (b) scans for UBF/LLDPE composites and first (c), and second (d) scans for BBF/LLDPE composites. The broad fusion range observed in the DSC curves presents a wide distribution of crystallite sizes of the LLDPE [23]. The melting behavior of LLDPE not only depends on the type and amount of comonomer, the

distribution of the short branches, but also to thermal history [24].

The second heating scans were used to determine the crystallinity index. The endothermic transition was characterized by noting the peak of melting endotherm (T_{m1} for first scan and T_{m2} for second scan), the heat of fusion (ΔH_{m1} for first scan and ΔH_{m2} for second scan) (calculated from the area under the melting peak) and the exothermic transition was characterized by noting the crystallization peak temperature (T_c), the crystallization enthalpies (ΔH_c) and the onset of melt crystallization (T_{omc}). The data are given in Table 2. Heat of fusion showed a significant increase in the second run which results from slower cooling in the DSC instrument. The dependency of crystallinity index (CI_{DSC}) of the LLDPE as a function of fiber (UBF/BBF) content was observed in an increasing trend in all composites presented in Table 2. This may be explained by introducing more structural regularities in crystal lattice. Drop in the crystallinity index by addition of 10–30% of BBF can be related to the change of the crystallinity behavior of LLDPE in the presence of BBF, compared to pure LLDPE. It proves the effect of BBF on the rate of nucleation and growth of spherulites. Shortening of solidification time in presence of filler can be probably the reason for reduction of crystallinity index of the composites, compared to pure LLDPE as observed by Sahebian et al. [25] in HDPE and nano-sized calcium carbonate system. The second reason of lower CI_{DSC} might be more compatible system when 10–30% BBF was used because hydrogen bond formation may be occurs between the fibers and thus, the surface energy of fibers become closer to the surface energy of the matrix.

Effects of BF on matrix crystallization

The effects of BF on the crystallization behavior of LLDPE were analyzed using non-isothermal DSC experiments.

Fig. 4 DSC melting curves of UBF/LLDPE (a, b) and BBF/LLDPE composites (c, d). Here a, c and b, d represent first and second scan, respectively
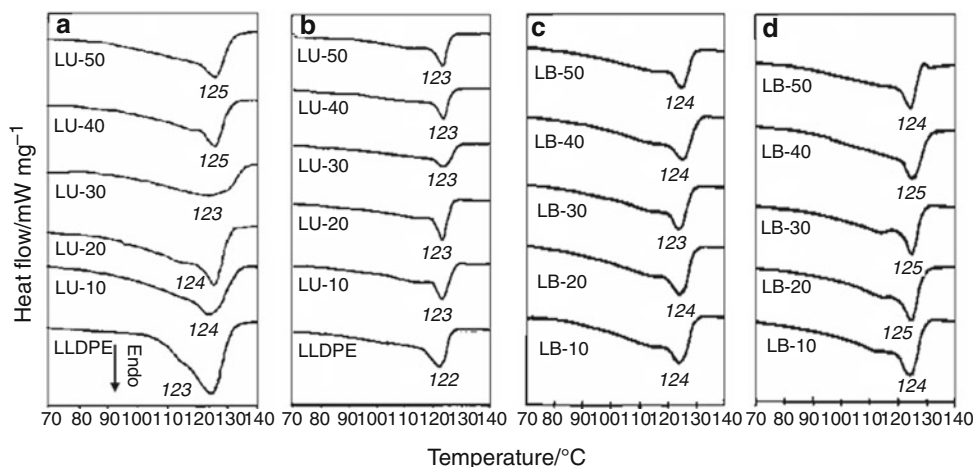
Table 2 DSC results of LLDPE composites

Samples	T_c/°C	$-\Delta H_c$/J g^{-1}	T_{omc}/°C	T_{m1}/°C	T_{m2}/°C	ΔH_{m1}/Jg^{-1}	ΔH_{m2}/Jg^{-1}	CI$_{DSC}$/%
LLDPE	101	78	106.76	123	121	66	80	56.89
LU-10	107	72	110.72	123	122	68	75	59.27
LU-20	107	64	111.27	124	122	64	68	60.45
LU-30	107	53	110.55	123	122	57	62	62.99
LU-40	107	51	110.80	124	122	54	55	65.20
LU-50	107	49	110.77	128	123	52	54	76.81
LB-10	107	63	111.21	124	123	63	66	52.15
LB-20	106	55	110.46	124	124	56	59	52.45
LB-30	107	53	111.75	125	123	55	56	56.89
LB-40	106	45	110.20	125	124	47	50	59.27
LB-50	107	46	110.86	124	123	44	46	65.43

Figure 5 shows the crystallization curves obtained for pure LLDPE and LLDPE/BF composites. The values of exothermal crystallization temperature peaks (T_c), the crystallization enthalpies (ΔH_c) are reported in Table 2. An increase in crystallization temperature (T_c) clearly would indicate that crystallization started earlier in the BF-filled composites than in the unfilled LLDPE. Zebarjad et al. found the similar results in the HDPE/CaCO$_3$ nanocomposite system [26].

It is possible to observe that the onset of melt crystallization (T_{omc}) takes place at higher temperatures in presence of the fibers, indicating a faster crystallization process, which is basically due to the heterogeneous nucleation of the fibers. There is not a substantial effect on the crystallization process with increasing the amount of fibers. A reduction of this effect with fiber treatments can be used as an indication of a good treatment. In fact, better

compatibility with the thermoplastic polyolefin can reduce the heterogeneous nucleation process and the consequent transcrystalline growth. Therefore, the CI$_{DSC}$ was lowered in the BBF/LLDPE composites. Moreover, it has been
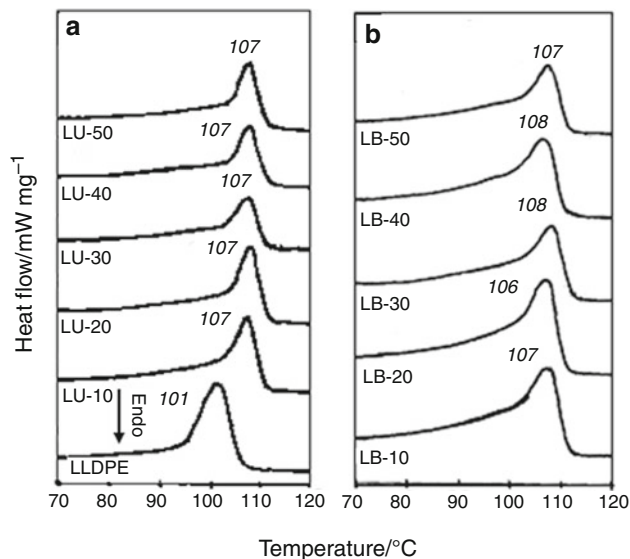
Fig. 5 Non-isothermal crystallization curves of UBF/LLDPE (**a**) and BBF/LLDPE composites (**b**) with varying fraction of BF
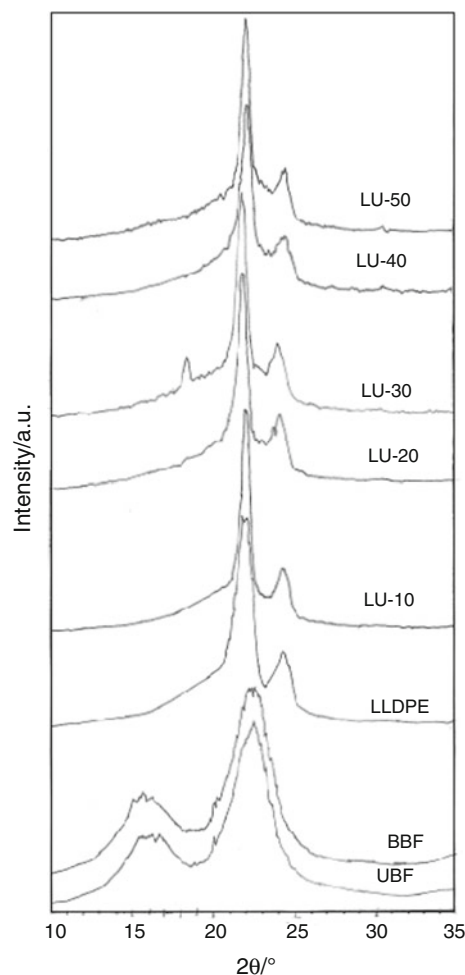
Fig. 6 X-ray diffraction patterns of bamboo-fiber, LLDPE, and their composites

shown that the physical modifications associated with the chemical treatment can play a key role in the development of transcrystallinity as the smoothing of the fiber surfaces. The various natural fibers such as bamboo can provide active sites on their surfaces to form the transcrystalline regions. Due to interaction of polymeric chains and the fiber surface, transcrystallinity can improve the adhesion of the fiber to the polymeric matrixes [27].

X-ray diffraction

X-ray diffractograms of LLDPE, UBF, BBF, and its composites are presented in Fig. 6. It has been reported that in cellulosic fibers the peaks at about 22° corresponded to the (0 0 2) lattice plane of cellulose [28]. In addition, the purified lignin shows broad peak at 14.8 and 21.7° [29]. In our composites the peak at 15° disappeared which could be due to reduction in absorption for lower density constituent such as BFs in the composites as it is dispersed in the matrix. Thicker fiber layers were to be needed to obtain peak. Yao et al. [30] in X-ray diffraction experiment showed that introduction of rice straw and wood fibers to virgin and recycled HDPE matrix did not change characteristic peak position as we found in our experiment.

The overall peak intensity as compared to pure LLDPE increased due to increase in the transcrystallinity (discussed in previous section). The peak intensity is directly dependent on the distribution of particular atoms in the structure and increase in peak intensity suggested the structural perfection. The relative decrease in intensity of

peaks in the composites can be connected to decrease in the crystalline structure. However, the intensity of the peaks did change, suggesting differences in crystallinity. Material crystallizes after addition of BF leading to a further sharpening of the peaks. The peaks broaden toward each other on addition of BF from 10 to 50%. This could be due to solid non-homogeneity. The values of the d spacing in all composites as given in Table 3 remain constant as found for LLDPE.

Table 3 XRD results of UBF composites

| Sample	Peak position	d_{spacing}	Peak height	χ_c/%
UBF	15.407	5.75130	72.8991	52.12
	22.798	3.90074	180.2512	
BBF	15.373	5.76385	100.0899	56.71
	22.588	3.93653	279.8288	
LLDPE	22.059	4.02972	241.9207	28.80
	24.423	3.64474	51.6578	
LU-10	22.004	4.03957	984.6397	30.78
	24.405	3.64742	281.8519	
LU-20	21.847	4.06834	707.5980	31.75
	24.271	3.66714	207.5013	
LU-30	21.894	4.05973	595.0264	31.90
	24.186	3.67985	155.2948	
LU-40	22.176	4.00869	577.4196	35.18
	24.474	3.63722	134.8131	
LU-50	22.168	4.01007	319.1715	39.89
	24.531	3.62889	93.0763	
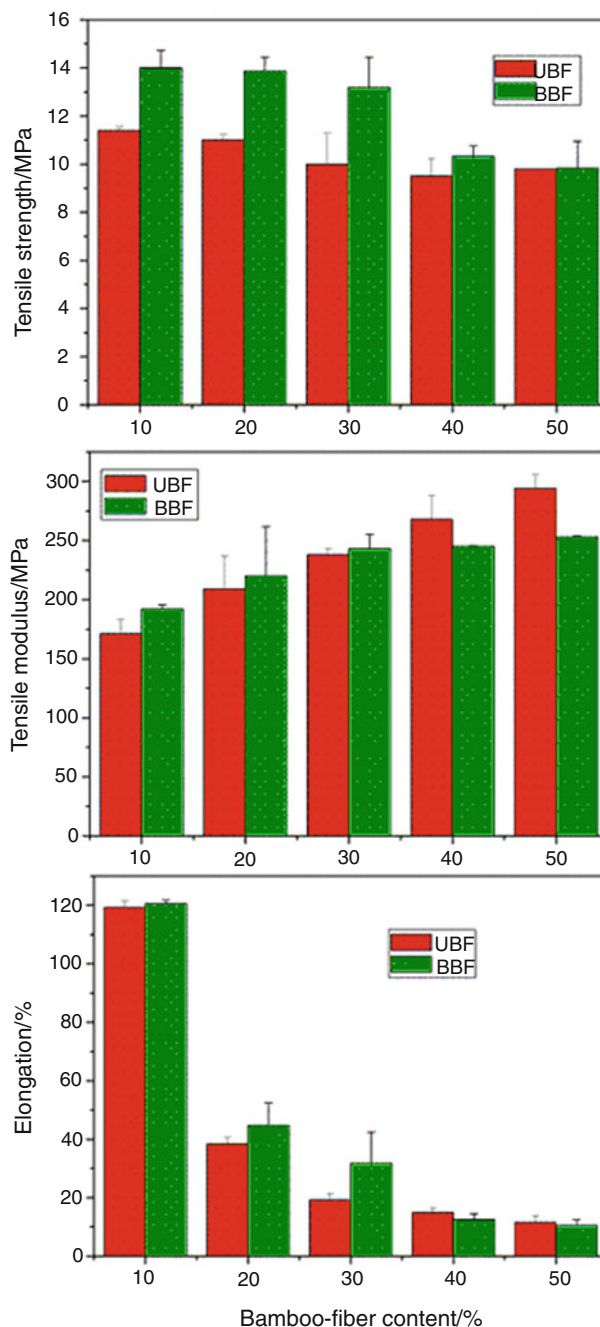
Fig. 7 Tensile properties of unbleached and bleached bamboo-fiber composites

Tensile properties

The tensile strength, modulus and elongation of pure LLDPE were found to be 19 MPa, 128 MPa, and 1079 (%), respectively. Figure 7 shows the comparison in the tensile properties of UBF and BBF reinforced LLDPE composites. The overall tensile strength of both types of composites was lower when compared to pure LLDPE because of the poor interfacial adhesion due to hydrophilic BF and hydrophobic LLDPE. The tensile strength was dropped by 40–53% in UBF and 26–48% in BBF composites. At higher loading of fibers, the tensile strength further reduced because of the probability of interfiber contact and thus the extent of aggregation was surely formed. At lower fraction of BF, the BBF composites showed higher tensile strength which may be attributed to greater physical interaction of BBF with LLDPE matrix. Tensile modulus increased from 34 to 130% in UBF composites and 50 to 97% in BBF composites as a function of fiber content. Up to 30% fiber content, BBF composites gave higher modulus than UBF composites but on further increasing the fiber content UBF gave high modulus value when compared to BBF composites. The similar up-down trend in modulus was reported by Chen et al. [31] and Thwe et al. [32] in BF–polypropylene composites without compatibilizer. The elongation decreased significantly upon incorporation of BF. This may be due to increase in the discontinuity of matrix with increase in disperse phase of BF. The higher content of BBF reduced the compatibility owing to the agglomeration of fibers.

Morphological characterization

Figure 8 shows the SEM photographs at ×100 magnification, of BF extracted by the delignification and bleaching methods. This photograph clearly indicates that the bundles were effectively separated into unbundled fibers and a very small amount of substances like lignin moiety, natural waxes, and pectins found in UBF remained on the surface of the UBF even after delignification under pressure was applied while in bleaching these materials dissoluted and gave more even rough surface of fiber. SEM photographs of LU/LB composites for fiber dispersion at a magnification of ×400 are shown in Fig. 9. It can be clearly seen from SEM that the agglomeration occurs at higher loading of fibers that may lead to low mechanical properties (Fig. 7) for composites at higher fiber loading. Large spaces were found at the points where the fibers were crossing. It is assumed that when the fibers are stacked on top of each other, the spaces are likely to be made at the crossover points because of their rigidity. The fibers pullout from the matrix shows the poor interfacial adhesion between fibers and the matrix. The BBF shows good compatibility with matrix as the lesser number of cavities was found in compared to LU composites which again justifies the use of BBF for the preparation of composites with high mechanical properties (Fig. 7).

The matrix wettability can be seen at higher magnification ×1.0 k for 30 mass% of fiber content. The matrix show moderately good wettability with the BBF in LB composites while almost no wettability was found with the UBF in LU composites as seen in Fig. 10. The spaces were also found near the UBF which shows poor physical attraction between UBF and matrix and that can be decreased by removing some water absorbing materials from the surfaces of UBF and making fiber rougher and even as we have shown in the case of bleached fiber (Fig. 10b).

Water uptake of composites

It is known that the interfacial adhesion between matrix and a natural fiber decreases due to water absorption which

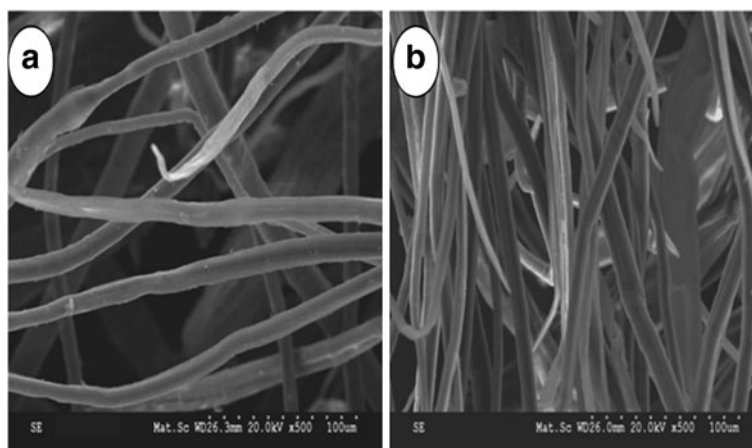**Fig. 8** SEM photographs of unbleached bamboo fibers (**a**) and bleached bamboo-fibers (**b**)

Fig. 9 SEM photographs to show the fiber dispersion in unbleached bamboo-fibers composites: (**a**) LU-10, (**b**) LU-30, (**c**) LU-50 and bleached bamboo-fiber composites: (**d**) LU-10, (**e**) LU-30, (**f**) LU-50
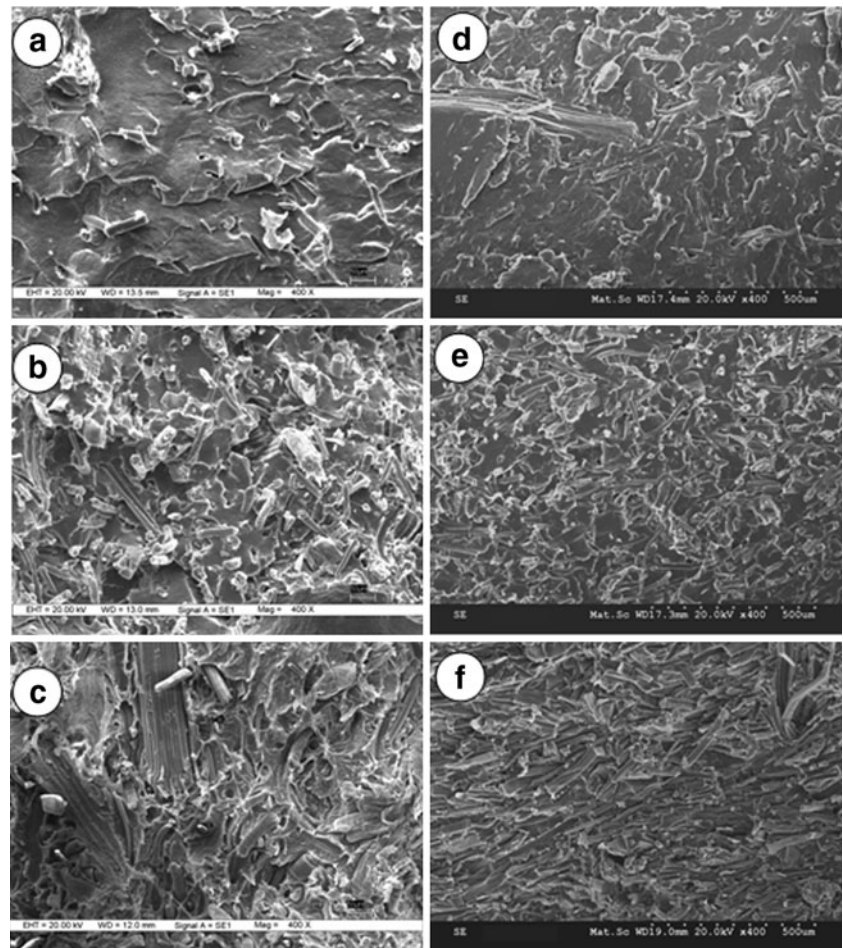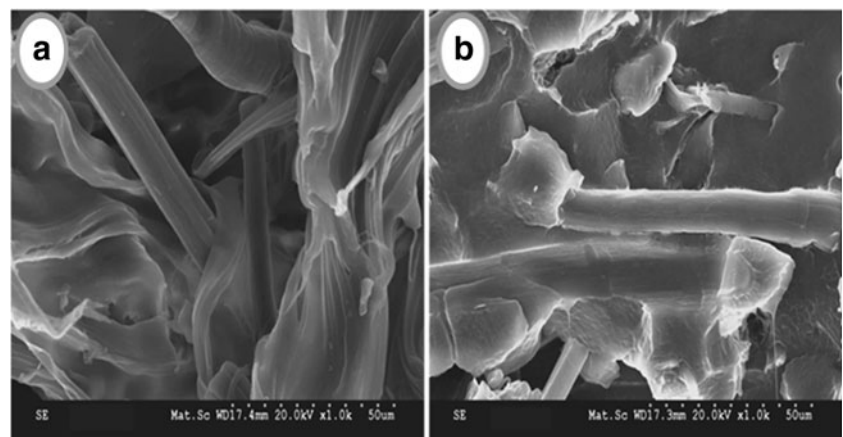

Fig. 10 SEM photographs of unbleached bamboo-fibers composite (**a**) and bleached bamboo-fiber composite (**b**) at 30% fiber content to show the compatibility

deteriorates the mechanical properties of composites [33]. Figure 11 shows the water sorption as a function of square root of soaking time (h). All the composites (LU/LB) attained a saturation level after 900 h. The water uptake of UBF composites were higher than that of BBF composites as water absorbing materials removed from the surface of UBF to produce BBF. As seen in morphological studies, there was a sufficient space near the UBF and hence, higher water uptake as compared to BBF. Hence, it is necessary to enhance the hydrophobicity of the BF by bleaching technique in order to develop composites with better mechanical properties and lower water uptake.
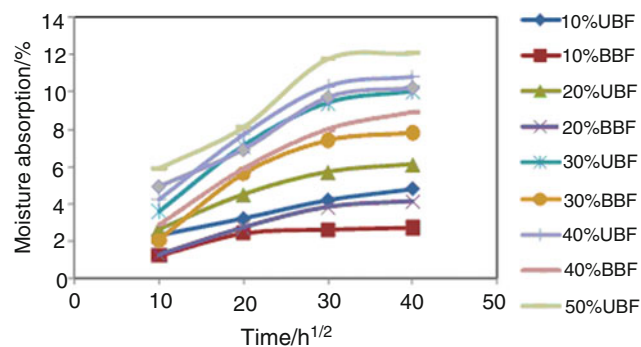
Fig. 11 Plots of water sorption of composites as a function of square root of time

Conclusions

The mentioned fiber extraction technique effectively separated fiber bundles into unbundled fiber. Our results suggested that the bleached fibers have more compatibility with matrix. During bleaching some materials (lignin moiety, natural waxes, and pectins found in cellulose fibers, etc.) of high water adsorption capacity might have been dissolved from the delignified fiber (UBF); hence BBF could uptake less water. This can be possible reason of a better compatibility of BBF as well as better wettability with the apolar matrix. The water sorption saturation level was lower for BBF composites as compared to UBF composites. The thermal and mechanical properties of BBF were also better than UBF composites which further support the benefit of using BBF as reinforcement materials. Due to well-known antifungal action of sodium chlorite, BBF-reinforced composites can have potential applications in food-processing industry.

References

1. Bledzki AK, Gassan J. Composite reinforced with cellulose based fibers. Prog Polym Sci. 1999;24:221–74.
2. Gassan J, Bledzki AK. Possibilities to improve the properties of natural fiber reinforced plastics by fiber modification–jute polypropylene composites. Appl Compos Mater. 2000;7:373–85.
3. Yoshida H, Zhang GZ, Kitamura T, Kawai T. Compatibility of polymer blends evaluated by crystallization dynamics: simultaneous DSC-FTIR method. J Therm Anal Calorim. 2001;64:577–83.
4. Mengeloglu F, Karakus K. Thermal degradation, mechanical properties and morphology of wheat straw flour filled recycled thermoplastic composites. Sensors. 2008;8:500–19.
5. Bouza R, Marco C, Ellis G, Martín Z, Gómez MA, Barral L. Analysis of the isothermal crystallization of polypropylene/wood flour composites. J Therm Anal Calorim. 2008;94:119–27.
6. Mengeloglu F, Kabakci A. Determination of thermal properties and morphology of eucalyptus wood residue filled high density polyethylene composites. Int J Mol Sci. 2008;9:107–19.
7. Awal A, Ghosh SB, Sain M. Thermal properties and spectral characterization of wood pulp reinforced bio-composite fibers. J Therm Anal Calorim. 2010;99:695–701.
8. Habibi Y, El-Zawawy WK, Ibrahim MM, Dufresne A. Processing and characterization of reinforced polyethylene composites made with lignocellulosic fibers. Compos Sci Technol. 2008;68:1877–85.
9. Yao F, Wu Q, Lei Y, Guo W, Xu Y. Thermal decomposition kinetics of natural fibers: activation energy with dynamic thermogravimetric analysis. Polym Degrad Stab. 2008;93:90–8.
10. Rao KMM, Rao KM. Extraction and tensile properties of natural fibers: Vakka, date and bamboo. Compos Struct. 2007;77:288–95.
11. Deshpande AP, Rao MB, Rao CL. Extraction of bamboo-fibers and their use as reinforcement in polymeric composites. J Appl Polym Sci. 2000;76:83–92.
12. Okubo K, Fujii T, Yamamoto Y. Development of bamboo-based polymer composites and their mechanical properties. Compos A. 2004;35:377–83.
13. Fengel D, Shao X. A chemical and ultrastructural study of the bamboo species Phyllostachys makinoi Hay. Wood Sci Technol. 1984;18:103–12.
14. Subramanian K, Senthil Kumar P, Jeypal P, Venkatesh N. Characterization of ligno-cellulosic seed Fiber from Wrightia Tinctoria plant for textile applications—an exploratory investigation. Eur Polym J. 2005;41:856–61.
15. Bosilevac JM, Shackelford SD, Fahle R, Biela T, Koohmaraie M. Decreased dosage of acidified sodium chlorite reduces microbial contamination and maintains organoleptic qualities of ground beef products. J Food Protect. 2004;67:2248–54.
16. Castillo A, Lucia LM, Kemp GK, Acuff GR. Reduction of Escherichia coli O157:H7 and Salmonella typhimurium on beef carcass surfaces using acidified sodium chlorite. J Food Protect. 1999;62:580–4.
17. Ransom JR, Belk KE, Sofos JN, Stopforth JD, Scanga JA, Smith GC. Comparison of intervention technologies for reducing Escherichia coli O157 H7 on beef cuts and trimmings. Food Protect Trends. 2003;23:24–34.
18. Singha AS, Thakur VK. Grewia optiva fiber reinforced novel, low cost polymer composites. e-J Chems. 2009;6:71–6.
19. Biagiotti J, Puglia D, Torre L, Kenny JM. A systematic investigation on the influence of the chemical treatment of natural fibers on the properties of their polymer matrix composites. Polym Compos. 2004;25:470–9.
20. Kim HS, Kim S, Kim HJ, Yang HS. Thermal properties of bio-flour-filled polyolefin composites with different compatibilizing agent type and content. Thermochim Acta. 2006;451:181–8.
21. Da Costa HM, Ramos VD. Analysis of thermal properties and rheological behavior of LLDPE/EPDM and LLDPE/EPDM/SRT mixtures. Polym Test. 2008;27:27–34.
22. Molya KA, Raduschb HJ, Androshb R, Bhagawanc SS, Thomasd S. Nonisothermal crystallisation, melting behavior and wide angle X-ray scattering investigations on linear low density polyethylene (LLDPE)/ethylene vinyl acetate (EVA) blends: effects of compatibilisation and dynamic crosslinking. Eur Polym J. 2005;41:1410–9.
23. Zang YH, Sapieha S. A differential scanning calorimetric characterization of the sorption and desorption of water in cellulose/linear low-density polyethylene composites. Polymer. 1991;32:489–92.
24. Qi M, Yao F, Zheng J, Qian R. Effect of thermal history on crystallization and melting behaviour of LLDPE. J Therm Anal Calorim. 1993;40:783–9.
25. Sahebian S, Zebarjad SM, Khaki JV, Sajjadi SA. The effect of nano-sized calcium carbonate on thermodynamic parameters of HDPE. J Mater Process Technol. 2009;209:1310–7.

26. Zebarjad SM, Sajjadi SA, Tahani M, Lazzeri A. A study on thermal behaviour of HDPE/CaCO₃ nanocomposites. J Achiev Mater Manuf Eng. 2006;17(1–2):173–6.

27. Araújo JR, Waldman WR, De Paoli MA. Thermal properties of high density polyethylene composites with natural fibers: coupling agent effect. Polym Degrad Stab. 2008;93:1770–5.

28. Lei Y, Wu Q, Yao F, Xu Y. Preparation and properties of recycled HDPE/natural fiber composites. Compos A. 2007;38:1664–74.

29. Sarkar S, Adhikari B. Synthesis and characterization of lignin-HTPB copolyurethane. Eur Polym J. 2001;37:1391–401.

30. Yao F, Wu Q, Lei Y, Xu Y. Rice straw fiber-reinforced high-density polyethylene composite: effect of fiber type and loading. Ind Crops Prod. 2008;28:63–72.

31. Chen X, Guo Q, Mi Y. Bamboo fiber-reinforced polypropylene composites: a study of the mechanical properties. J Appl Polym Sci. 1998;69:1891–9.

32. Thwe MM, Liao K. Effects of aging on the mechanical properties of bamboo-glass fiber reinforced polymer matrix hybrid composites. Compos A. 2002;33:43–52.

33. Buehler FU, Seferis JC. Effect of reinforcement and solvent content on moisture absorption in epoxy composite material. Compos A. 2000;31:741–8.